Chapter 36
Soft Tissue Characterisation Using a Force Feedback-Enabled Instrument for Robotic Assisted Minimally Invasive Surgery Systems

Mohsen Moradi Dalvand, Bijan Shirinzadeh, Saeid Nahavandi, Fatemeh Karimirad and Julian Smith

Abstract An automated laparoscopic instrument capable of non-invasive measurement of tip/tissue interaction forces for direct application in robotic assisted minimally invasive surgery systems is introduced in this chapter. It has the capability to measure normal grasping forces as well as lateral interaction forces without any sensor mounted on the tip jaws. Further to non-invasive actuation of the tip, the proposed instrument is also able to change the grasping direction during surgical operation. Modular design of the instrument allows conversion between surgical modalities (e.g., grasping, cutting, and dissecting). The main focus of this paper is on evaluation of the grasping force capability of the proposed instrument. The mathematical formulation of fenestrated insert is presented and its non-linear behaviour is studied. In order to measure the stiffness of soft tissues, a device was developed that is also described in this chapter. Tissue characterisation experiments were conducted and results are presented and analysed here. The experimental results verify the capability of the proposed instrument in accurately measuring grasping forces and in characterising artificial tissue samples of varying stiffness.

Keywords Actuation mechanism · Force measurement · Laparoscopic instrument · Modularity · Power transmission mechanism · Robotic assisted minimally invasive surgery (RAMIS) · Strain gages

M. M. Dalvand (✉) · S. Nahavandi · F. Karimirad
Centre for Intelligent Systems Research (CISR), Deakin University, Waurn Ponds Campus, Melbourne, VIC 3216, Australia
e-mail: mohsen.m.dalvand@deakin.edu.au

B. Shirinzadeh
Robotics and Mechatronics Research Laboratory (RMRL), Department of Mechanical and Aerospace Engineering, Monash University, Melbourne, Australia

J. Smith
Department of Surgery, Monash Medical Centre, Monash University, Melbourne, Australia

H. K. Kim et al. (eds.), *Transactions on Engineering Technologies*,
DOI: 10.1007/978-94-017-9115-1_36,

1 Introduction

Having improved the disadvantages of the traditional laparoscopic surgery, Robotic Assisted Minimally Invasive Surgery (RAMIS) has negatively affected the surgeon's ability in palpating and diagnosing soft tissues of varying stiffness during surgery [1, 2]. The lack of force feedback has motivated several researchers to explore possible methods of restoring this feature to RAMIS by making laparoscopic instruments capable of measuring tip/tissue interaction forces. Strain gauges were applied on the tip and handle of laparoscopic surgical forceps to characterise tissues [3–6]. Retrofitting of laparoscopic forceps with a commercial six-axis force/torque sensor encapsulated in the instrument shaft [7] and a force sensor on the handle of the tool [8] were studied. A two Degree Of Freedom (DOF) force sensing sleeve for 5 mm laparoscopic instruments was developed with advantages of compatibility and modularity among several types of surgical instruments [9].

A micro-machined piezoelectric tactile sensor embedded beneath silicon teeth of the grasper jaws was developed that has some disadvantages including ability to measure only dynamic forces, susceptibility to damage from shear forces, non-sterilizability, and high cost [10]. At more complex level, a distal force/torque sensor for laparoscopic instruments was developed that uses Stewart platform to locate six strain gauges for measuring forces and torques along all of its six measurement axes [11, 12]. Preliminary results on design and fabrication of a cutting tool with an integrated tri-axial force sensor to be applied in fetal surgery procedures were reported [13, 14]. A miniature uniaxial force sensor for use within a beating heart during mitral valve annuloplasty was presented [15].

Besides retrofitting conventional laparoscopic instruments, research efforts have also been conducted in developing automated laparoscopic tools with force measurement capability [16, 17]. Most of these tools incorporate the advantage of actuation mechanisms for utilising in robotic surgical systems [18, 19]. Further to the force sensing laparoscopic instruments, robotic surgical systems were proposed with force measurement capabilities including Black Falcon [20] and Blue-DRAGON [21]. The possibility of using a trocar sensor for measurement of the surgical forces was also investigated in a robotic surgical system [22]. Although these research efforts were steps toward introducing force-feedback in robotic assisted surgical systems, there still exist many problems within the designs of surgical tools and their use in robotic surgery including modularity, size and force measurement issues.

In this chapter, an automated modular laparoscopic instrument is introduced that provides tool/tissue interaction force measurement capability directly from the surgery site [2, 23]. The proposed instrument is presented in Fig. 1 and different components of it are highlighted in this figure. The proposed instrument is incorporated with a micropositioning parallel manipulator and the RCM control algorithms has already been developed and evaluated [24–26]. The rest of the chapter is organized into three sections. In the next section, the modelling and

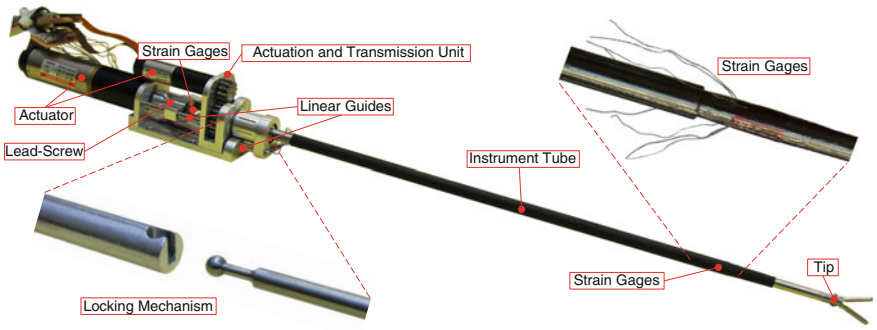

Fig. 1 Proposed force feedback-enabled minimally invasive surgery instrument

development of the proposed instrument are described that cover modularity feature, force sensing capability and modelling of tool tip. In Sect. 3, a device developed to measure stiffness of soft tissues is described. Experimental results are also presented in this section to verify the capabilities of the proposed instrument in probing and characterising soft tissues. Concluding remarks are made in Sect. 4.

2 Modelling and Development

2.1 Interchangeability Feature

Interchangeability feature of the proposed instrument enables the operator to easily and quickly change between variety of laparoscopic insert types e.g., grasping, cutting, and dissecting without loss of the force sensing capability. A stainless steel tube with 7 mm in diameter and 33 cm in length was designed in the way that it can be fitted concentrically, like a sleeve, over any 5 mm insert type manufactured by Matrix Surgical company. The nut (Fig. 2) couples the sleeve and the insert assembled to it to the base module. To minimise any potential error caused by unwanted clearance in the assembly, a part called nut-base was designed that is attached to the nut using a ball-bearing. Fastening the nut slides two supportive guides (Fig. 2) incorporated to the base inside two holes of the nut-base supporting the long tube of the instrument (Fig. 2). By help of this nut, insert, long tube and base module can be quickly disassembled and the insert type can be converted to the variety of insert types available.

Two actuators from Maxon Motor company were employed to actuate two DOFs related to the tip direction and operation (Fig. 2). Transmission and conversion of power required to change grasping direction and to operate tip jaws were achieved by spur gears and a lead-screw mechanism (Fig. 2). The size of the screw used in the lead-screw mechanism is *M*6 with 1 mm pitch. The mechanism to lock the insert to the lead-screw is also shown in Fig. 1.

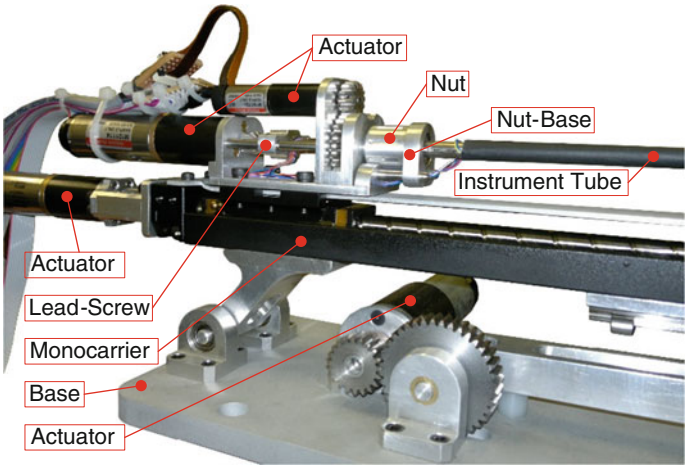

Fig. 2 The proposed instrument incorporated with a four-bar mechanism in a robotic assisted surgery system [25]

2.2 Force Measurement

In the proposed instrument, surface strains of the lead of the lead-screw mechanism is measured as a quantity for the normal grasping forces applied to the soft tissue at tip jaws. Two strain gages were embedded in the lead-screw mechanism (Fig. 1) to measure tension and compression strains in the lead of the lead-screw representing the normal grasping forces. Calibrations of the strain gage configurations were performed using known masses.

2.3 Kinematics of Grasping Mechanism

Pivotal mechanism are utilised at the tip jaws of most of the laparoscopic surgical instruments. The pivotal motion is commonly generated by linear displacement of the push rod and a mechanism to convert it to rotary displacement. In the proposed instrument the required linear movement is produced by a rotary actuator coupled with a lead-screw mechanism. Figure 3 describes the kinematics parameters of the tip mechanism for two different states where the tip is closed and tip jaws are at an arbitrary angle θ. In order to control the actuated laparoscopic instrument, it is necessary to obtain the relationship between the angular position of jaws (θ) and angular rotation of the gearbox shaft (ϕ). Considering Fig. 3, the following equations are derived:

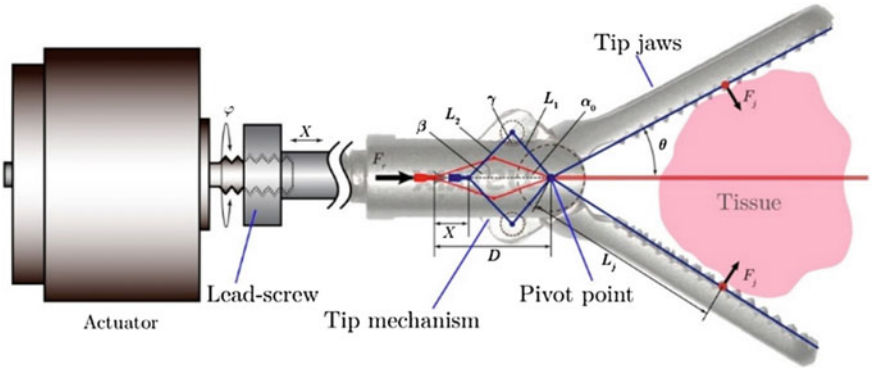

Fig. 3 Kinematics parameters of the tip mechanism for two different states of tip jaws

$$\alpha = \alpha_0 + \theta \tag{1}$$

$$L_1 \sin(\alpha) - L_2 \sin(\beta) = 0 \tag{2}$$

$$L_1 \cos(\alpha) + L_2 \cos(\beta) = D - X \tag{3}$$

where L_1 and L_2 are the constant geometrical parameters of the tip mechanism, α, β, and X are the variables of the mechanism and α_0 and D are the variables of the mechanism where the tip is at closed state ($\theta = 0$) as described in Fig. 3. Combining Eqs. (2) and (3) yields:

$$\alpha + \beta = A \tag{4}$$

where A is as follows:

$$A = Arc\cos\left(\frac{(D-X)^2 - L_1^2 - L_2^2}{2L_1L_2}\right) \tag{5}$$

Moreover, using Eqs. (2) and (4), α can be determined as follows:

$$\alpha = Arc\sin\left(\sqrt{\frac{L_2^2\sin^2(A)}{L_2^2\sin^2(A) + (L_1 + L_2\cos(A))^2}}\right) \tag{6}$$

Using Eqs. (1), (5) and (6), and considering $X = \phi/2\pi$ for any angular position of the gearbox shaft (ϕ), the jaw's angular position is obtained as follows:

$$\theta = Arc\sin\left(\frac{\sqrt{\left[4L_1^2L_2^2 - \left((D - \frac{\phi}{2\pi})^2 - L_1^2 - L_2^2\right)^2\right]}}{4L_1(D - \frac{\phi}{2\pi})}\right) - \alpha_0 \tag{7}$$

To be able to control tip jaws to any specific angular position, the angular position of the gearbox shaft (ϕ) need to be derived as a function of the tip angular position (θ). This mathematical relation is derived as follows:

$$\phi = 2\pi(\sqrt{L_2^2 - L_1^2 \sin(\alpha_0 + \theta)^2} - L_1 \cos(\alpha_0 + \theta) - D) \tag{8}$$

According to the nonlinear relationship between θ and ϕ, the response of the tip with relatively closed jaws to the actuator shaft displacements is faster than that of the tip with relatively opened jaws. Strain gages applied to the lead rod results in the measurement of the tension and compression forces of the rod that is marked by F_r in Fig. 3. In order to determine the actual forces applied to the tissue at the tip jaws (F_j), the force propagation of the tip mechanism (the relation between F_r and F_j) should be defined.

It is worth noting that for the sake of modelling of the force propagation, the force applied to the tissue is assumed to act at a point lying at a distance L_j from the pivot point of the tip [12, 27, 28]. Neglecting the friction and balancing the forces and the moments around the pivot point leads to the derivation of the force propagation model as follows:

$$F_j = \frac{L_1}{2L_j} \times \frac{\sin(\gamma)}{\cos(\beta)} \times F_r \tag{9}$$

where γ is the angular variable of the mechanism (Fig. 3) and variables β and γ are defined using the following equations:

$$\beta = arc\sin(\frac{L_1 \sin(\theta + \alpha_0)}{L_2}) \tag{10}$$

$$\gamma = \pi - (\theta + \alpha_0) - \beta \tag{11}$$

The ratio of the forces in the push rod and at tip jaws (F_r/F_j) with respect to jaws angular positions indicates that applying a force to the push rod generates greater force at the jaws with relatively small angular position in comparison with the force that it generates at the jaws with relatively large angular position. Closing the tip jaws increases the normal forces of the jaws with the rate higher than that of the decrease in the angular position of the jaws.

The nonlinear relationship between θ and ϕ and also F_r/F_j for the allowable range of movements of the tip jaws is plotted in Fig. 4. As this figure indicates, applying a force to the push rod generates greater force at the jaws with relatively small angular position in comparison with the force that it generates at the jaws with relatively large angular position. Closing the tip jaws increases the normal forces of the jaws with the rate higher than that of the decrease in the angular position of the jaws.

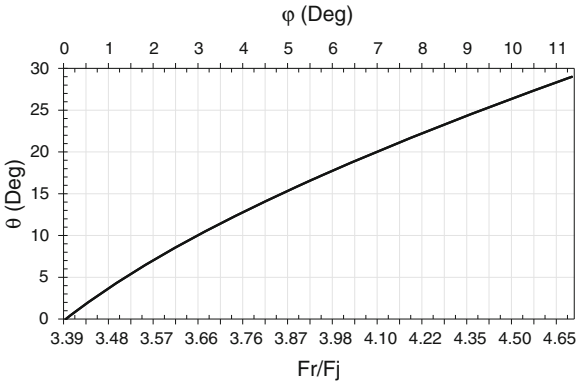

Fig. 4 Nonlinear relationships of θ with ϕ and F_r/F_j

3 Experimental Results

3.1 Stiffness Measurement

The Young's modulus is a measure of the stiffness of an elastic material and is a quantity used to characterize materials. An indentation experiment was conducted in this research to compute the effective Young's moduli of artificial tissue samples and study their mechanical properties relative together assuming linear elasticity. The assumption of linear elasticity relies on the applying of small indentation relative to the characteristic dimensions of the tissues. The effective elastic Young's modulus (E) corresponding to an indentation depth of δ may be calculated as follows [29]:

$$E = \frac{3F}{8d\delta} \tag{12}$$

where F is the reaction force and d is the diameter of a circular punch indenter applied to the soft tissue.

To conduct the experiment, a high-precision instrument was developed (Fig. 5) by retrofitting a micrometre with position resolution of 0.01 mm with a FSG-15N1A force sensor from Honeywell Sensing and Control (1985 Douglas Drive North Golden Valley, MN 55422 USA) with the force resolution of 1 gr. The instrument was used to apply precise indentations to the tissue samples and record the force responses using a U6 data acquisition (DAQ) module from LabJack Corporation (3232 S Vance St STE 100 Lakewood, CO 80227 USA) for three cycles per tissue sample. The average values were calculated and force-displacement relationships were obtained that are presented in Fig. 5.

The young modulus of the three selected soft tissues (Fig. 5) were calculated using Eq. (12) as 10.5, 17.7, and 26.0 kPa. These artificial tissue samples were deliberately chosen to be relatively close in terms of stiffness. They are also

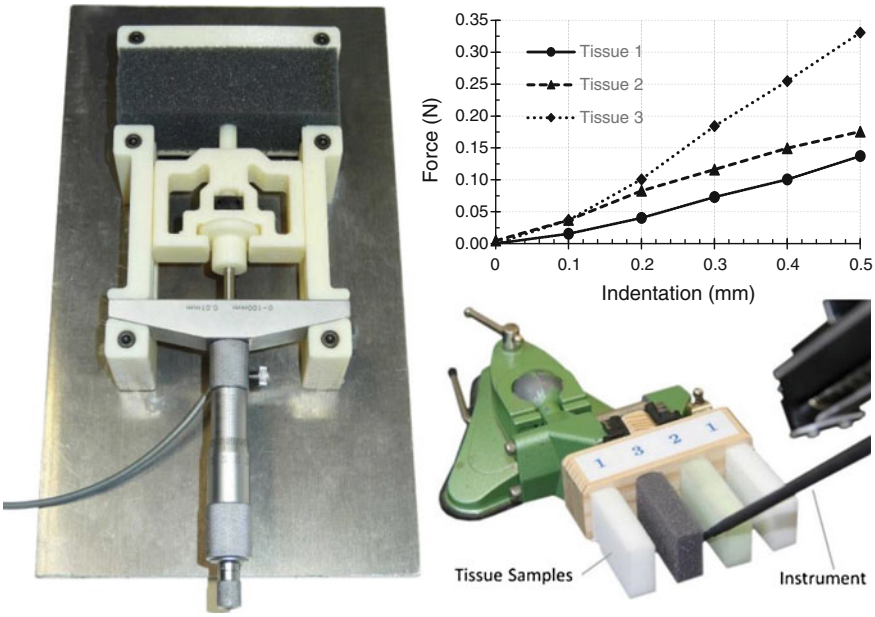

Fig. 5 The developed high-precision indentation device for stiffness measurement of soft tissue (*left*), force/displacement relationships (*right-top*) for the three selected artificial tissue samples made up of sponges (*right-bottom*)

selected to be representative of relatively softer tissues among human soft tissues with the range of young modulus from 0.1 to 241 kPa [30, 31]. These selections were made in order to properly evaluate the effectiveness of the proposed instrument in characterizing soft tissues with low and relatively close young moduli. These tissue samples were also examined by the surgeon collaborator to make a realistic choice of human soft tissues in the experimental studies.

3.2 Tissue Characterization Experiment

This experiment was conducted to evaluate the capability of the proposed instrument in non-invasive measurement of the grasping forces for tissue samples of varying stiffness. Three artificial tissue samples made up of sponge material that are identical in thicknesses but slightly different in stiffness were chosen for this experiment. In order to verify the accuracy of the measurement methodology as well as the correctness and the effectiveness of the post-processing algorithm, even in characterizing tissues with close stiffness, the tissues were purposely selected with slight variation in stiffness (Fig. 5), such that they would be hardly differentiated by direct exploration with one's fingers.

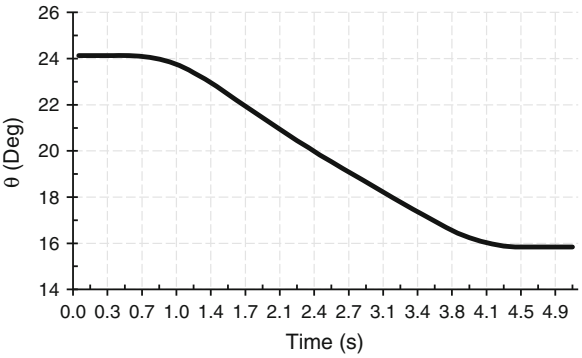

Fig. 6 Angular displacement of the tip jaws in the experiment

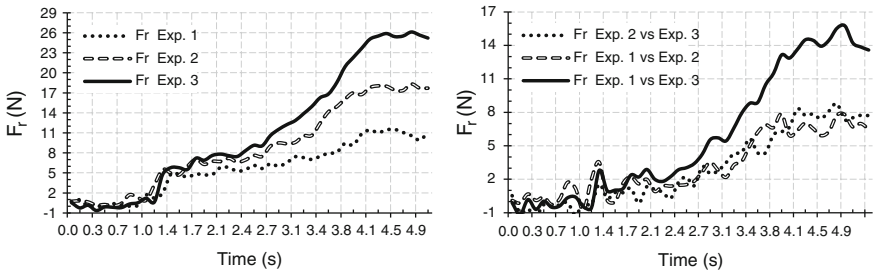

Fig. 7 Measured forces (*left*) and comparatives of the measured forces (*right*) applied to the push rod (F_r) in the experiment

In this experiment, according to the tip jaws angular displacements illustrated in Fig. 6, the tip jaws were closed from 24° to 16° while the tissue samples were grasped and the applied force to the push rod were measured using the strain gages applied to the lead-screw (Fig. 1). The initial positions of the tissue samples between jaws were held constant, therefore they all were incurred similar deformation but with different normal forces. The data acquired in this experiment are plotted in Fig. 7. This figure shows the measured forces applied to the push rod (F_r). In the real palpation, for the purpose of diagnosing the normal/infected tissues, usually comparative forces/stiffness of the tissues are of interest. Therefore, the comparatives between the measured forces applied to the push rod for the three different tissues are also calculated and are also plotted in Fig. 7. The normal forces applied to the tissues at tip jaws calculated using Eq. (9) as well as the comparatives between these forces are plotted in Fig. 8. According to the Figs. 6, 7 and 8, the jaws started to close at the initial angular position of 24° at time 0.7 s and reached the final position of 16° at time 4.3°.

Compression started at time 1.2 s with tip jaws in angular position of 23.2° where the recorded data showed a sudden increase in grasping forces. As the jaws were closing, the grasping forces were increasing but with higher rate for harder

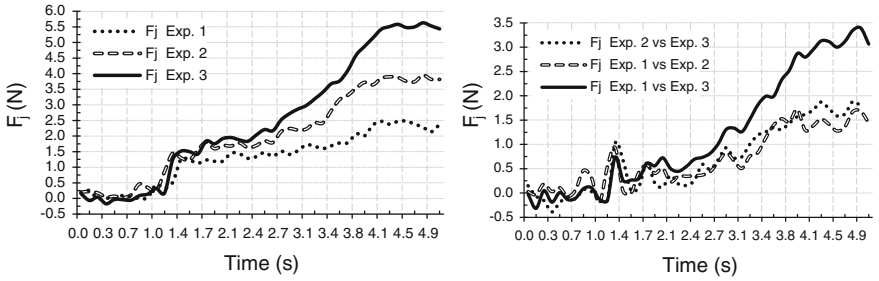

Fig. 8 Calculated forces (*left*) and comparatives of the calculated forces (*right*) applied to the artificial tissue samples (F_j) in the experiment

tissue than the rate for softer tissue. Once the jaws got to the final position at time 4.3 s, the forces remained constant to the maximum grasping forces. In this experiment, the measured peak forces applied to the push rod of the insert for three tissue samples from softer to harder are 12, 18, and 26 N, respectively.

These forces are, respectively, equivalent to 2.5, 3.8, and 5.6 N of the calculated normal forces at jaws directly applying to the tissue (Fig. 8). As it is also observed from the Figs. 7 and 8, the differences between increase rates of F_j and F_r increased as jaws were closing, got to the maximum difference at time 2.4 s where the jaws were at 20°, and decreased to its minimum value in this experiment when the tip was at its closest state of 16°. This phenomenon confirms the nonlinear relationship of F_j and F_r or the angular position of tip jaws (θ) with the angular displacement of the actuator shaft (ϕ) as it is also presented in Fig. 4. As it is shown in Figs. 7 and 8, there is a jump in all of the comparative forces at the time 1.4 s where the compression is started which is verify the effectiveness of the proposed instrument in correctly measuring the grasping forces for different tissue sample specifically at the time of the compression where the magnitude of the grasping forces are in the lower range. As it is also clear from the Figs. 7 and 8, the measured forces using the proposed instrument are easily distinguishable which results in ability to characterise soft tissues of varying stiffness. Therefore, it can be concluded that the proposed laparoscopic instrument has good accuracy and performance for the grasping force measurement and is able to distinguish between tissues of varying stiffness even with relatively close young moduli.

4 Conclusion and Future Works

An automated minimally invasive surgical instrument was introduced, the modelling and development issues were discussed, and experimental results were presented and analysed in this paper. The proposed surgery instrument has the capability of minimally invasively measuring normal tip interaction forces e.g. grasping and cutting. The instrument features non-invasive actuation of the tip and

also the measurement of interaction forces without using any actuator and sensors at the jaws. The grasping direction in the proposed instrument can also be adjusted during the surgical procedure. The modularity feature of this force feedback-enabled minimally invasive instrument makes it interchangeable between various tool tips of all functionalities (e.g. cutter, grasper, and dissector) without loss of control and force measurement capability necessary to avoid tissue damage and to palpate and diagnose tissue and differentiate its stiffness during surgery. A high precision device for the measurement of young modulus of soft tissues were developed and utilised in this research. Experiments were conducted to evaluate capabilities of the proposed instrument in non-invasively measuring normal grasping forces. The result showed high accuracy and performance and verified the ability of the instrument in measuring normal grasping forces and in distinguishing between tissue samples even with slight differences in stiffness. The sterilizability of the instrument and especially the force sensing sleeve also needs improvements in future works before it can be used in surgery operating room.

Acknowledgement This research is funded by Australian Research Council, ARC Discovery-DP0986814, ARC LIEF-LE0668508, and ARC LIEF-LE0453629.

References

1. A.R. Lanfranco, A.E. Castellanos, J.P. Desai, W.C. Meyers, Robotic surgery: a current perspective. Ann. Surg. **239**, 14 (2004)
2. M. Moradi Dalvand, B. Shirinzadeh, J. Smith, Effects of realistic force feedback in a robotic assisted minimally invasive surgery system. Minimally Invasive Therapy and Allied Technologies (MITAT) (2013) (in press)
3. S.M. Sukthankar, N.P. Reddy, Towards force feedback in laparoscopic surgical tools, in *Proceedings of the 16th Annual International Conference of the IEEE Engineering in Medicine and Biology Society, 1994. Engineering Advances: New Opportunities for Biomedical Engineers.* IEEE (1994)
4. C.E. Reiley et al., Effects of visual force feedback on robot-assisted surgical task performance. J. Thorac. Cardiovasc. Surg. **135**, 196–202 (2008)
5. M. Fakhry, F. Bello, G.B. Hanna, A real-time compliance mapping system using standard endoscopic surgical forceps. IEEE Trans. Biomed. Eng. **56**, 1245–1253 (2009)
6. P. Lamata et al., Understanding perceptual boundaries in laparoscopic surgery. IEEE Trans. Biomed. Eng. **55**, 866–873 (2008)
7. P. Dubois, Q. Thommen, A.C. Jambon, In vivo measurement of surgical gestures. IEEE Trans. Biomed. Eng. **49**, 49–54 (2002)
8. J. Rosen, B. Hannaford, C.G. Richards, M.N. Sinanan, Markov modeling of minimally invasive surgery based on tool/tissue interaction and force/torque signatures for evaluating surgical skills. IEEE Trans. Biomed. Eng. **48**, 579–591 (2001)
9. S.K. Prasad et al., in *Medical Image Computing and Computer-Assisted Intervention*, pp. 279–286
10. J. Dargahi, M. Parameswaran, S. Payandeh, A micromachined piezoelectric tactile sensor for an endoscopic grasper: theory, fabrication and experiments. J. Microelectromech. Syst. **9**, 329–335 (2000)
11. U. Seibold, B. Kuebler, G. Hirzinger, Prototype of instrument for minimally invasive surgery with 6-axis force sensing capability, in *ICRA* (2005)

12. B. Kuebler, U. Seibold, G. Hirzinger, Development of actuated and sensor integrated forceps for minimally invasive robotic surgery. Int. J. Med. Robot. Comput. Assist. Surg. **1**, 96–107 (2005)
13. P. Valdastri et al., Integration of a miniaturised triaxial force sensor in a minimally invasive surgical tool. IEEE Trans. Biomed. Eng. **53**, 2397–2400 (2006)
14. M. Mahvash et al., Modeling the forces of cutting with scissors. IEEE Trans. Biomed. Eng. **55**, 848–856 (2008)
15. M.C. Yip, S.G. Yuen, R.D. Howe, A robust uniaxial force sensor for minimally invasive surgery. IEEE Trans. Biomed. Eng. **57**, 1008–1011 (2010). doi:10.1109/tbme.2009.2039570
16. J. Rosen, B. Hannaford, M.P. MacFarlane, M.N. Sinanan, Force controlled and teleoperated endoscopic grasper for minimally invasive surgery-experimental performance evaluation. IEEE Trans. Biomed. Eng. **46**, 1212–1221 (1999)
17. G. Tholey, J.P. Desai, A modular, automated laparoscopic grasper with three-dimensional force measurement capability, in *IEEE International Conference on Robotics and Automation.* IEEE (2007)
18. C.R. Wagner, N. Stylopoulos, R.D. Howe, The Role of Force Feedback in Surgery: Analysis of Blunt Dissection, in *Symposium on Haptic Interfaces for Virtual Environment and Teleoperator Systems* (2002)
19. M. MacFarlane, J. Rosen, B. Hannaford, C. Pellegrini, M. Sinanan, Force-feedback grasper helps restore sense of touch in minimally invasive surgery. J. Gastrointest. Surg. **3**, 278–285 (1999)
20. A.J. Madhani, G. Niemeyer, J.K. Salisbury, The black falcon: a teleoperated surgical instrument for minimally invasive surgery, in *Proceedings on 1998 IEEE/RSJ International Conference on Intelligent Robots and Systems*, vol. 2. IEEE (1998)
21. J. Rosen, J.D. Brown, L. Chang, M.N. Sinanan, B. Hannaford, Generalized approach for modeling minimally invasive surgery as a stochastic process using a discrete Markov model. IEEE Trans. Biomed. Eng. **53**, 399–413 (2006)
22. S. Shimachi, Y. Hakozaki, T. Tada, Y. Fujiwara, Measurement of force acting on surgical instrument for force-feedback to master robot console, in *International Congress Series*, vol. 1256. Elsevier (2003)
23. M. Moradi Dalvand, B. Shirinzadeh, S. Nahavandi, F. Karimirad, J. Smith, in *Lecture Notes in Engineering and Computer Science: Proceedings of The World Congress on Engineering and Computer Science*, WCECS 2013, pp. 419–424 (2013)
24. M. Moradi Dalvand, B. Shirinzadeh, Forward kinematics analysis of offset 6-RRC̄RR parallel manipulators, in *Proceedings of the Institution of Mechanical Engineers, Part C: Journal of Mechanical Engineering Science* **225**, 3011–3018 (2011)
25. M. Moradi Dalvand, B. Shirinzadeh, Motion control analysis of a parallel robot assisted minimally invasive surgery/microsurgery system (PRAMiSS). Robot. Comput.-Integr. Manuf. **29**, 318–327 (2013). doi:10.1016/j.rcim.2012.09.003
26. M. Moradi Dalvand, B. Shirinzadeh, Remote centre-of-motion control algorithms of 6-RRCRR parallel robot assisted surgery system (PRAMiSS), in *IEEE International Conference on Robotics and Automation (ICRA)*, IEEE (2012)
27. T. Hu, A. Castellanos, G. Tholey, J. Desai, Real-time haptic feedback in laparoscopic tools for use in gastro-intestinal surgery, in *Medical Image Computing and Computer-Assisted Intervention—MICCAI,* pp. 66–74 (2002)
28. M. Tavakoli, R. PateI, M. Moallem, in *Proceedings of IEEE International Conference on Robotics and Automation*, ICRA'04, pp. 371–376 (2004)
29. M.J. Uddin, Y. Nasu, K. Takeda, S. Nahavandi, G. Capi, An autonomous trimming system of large glass fiber reinforced plastics parts using an omni-directional mobile robot and its control, in *Proceedings: Eight International Conference on Manufacturing and Management: Operations Management and Advanced Technology: Integration for Success*. PCMM (2004)
30. S.B. Kesner, R.D. Howe, Position control of motion compensation cardiac catheters. IEEE Trans. Robot. **27**, 1045–1055 (2011)
31. S.G. Yuen, N.V. Vasilyev, P.J. del Nido, R.D. Howe, Robotic tissue tracking for beating heart mitral valve surgery. Med. Image Anal. **17**, 1236–1242 (2013)